

## 7B.3 Composite Analysis of Environmental Conditions Favorable for Significant Tornadoes across Eastern Kansas

Joshua M. Boustead<sup>1</sup>, and Barbara E. Mayes  
NOAA/NWS WFO Omaha/Valley, NE

William Gargan, George Phillips, and Jared Leighton  
NOAA/NWS WFO Topeka, KS

### 1. INTRODUCTION

Significant advancements have been made since the 1950s in the forecasting and warning for severe local storms. The widespread use of Doppler radar within the National Weather Service since the late 1990s has helped increase in the probability of detection of severe local storms producing flash flooding, large hail, damaging winds, and tornadoes. This, along with public education, has led to a significant drop in tornado related deaths since the 1950s. Nevertheless, anticipating the occurrence of significant events even in the first 24 hours continues to be a challenge to operational forecasters at times. The forecasting of hazardous weather continues to be a very important part of the thunderstorm warning process. The better forecasters are at identifying potentially significant events, the more lead time can be giving to users and the public about their potential. In addition, knowledge of the potential significance of an event can help forecasters better plan for staffing levels to meet the needs of the customers.

This study looks at one aspect of severe local storms forecasting, that of significant tornadoes (EF2 or greater) across eastern Kansas (Fig. 1). Although the precise mechanisms that lead to the development of a tornado are still unclear to some degree, operational experience indicates they frequently occur along either mesoscale boundaries, or within the warm sector of a synoptic scale extratropical cyclone where significant ambient low-level vorticity exists.

There are several goals to this study. The first goal is to create a composite of the synoptic environment associated with significant tornadoes that occur both with and without discernable surface boundaries, providing forecasters mental maps to utilize in anticipation of tornadic activity. The second goal is to develop a climatology of significant tornadoes in eastern Kansas, including favored time of day, distribution through the convective season, and other details useful to operational forecasters. Third, this study will look at the thermodynamic and wind shear environment associated with significant tornadoes occurring in Kansas, again both with and without discernable surface

boundaries, while developing statistics associated with their occurrence. Finally, this study will examine how the synoptic environment changes during the warm season.

### 2. DATA AND METHODOLOGY

A list of significant tornadoes was compiled using Storm Data (NCDC 1979-2007) from 1979 through 2007 for a part of eastern Kansas (Fig. 1). Observed surface data was obtained and then plotted using the Digital Atmosphere program. Subjective surface analyses were completed for each of the tornado occurrences 1 hour prior to 1 hour post tornado occurrence. Tornadoes were grouped in two different categories; ones occurring within 50 km of a discernable (subjectively analyzed) surface boundary and tornadoes occurring without any discernable surface boundary.

Once compiled, it was noted that a number of the tornado days contained multiple significant tornadoes. To reduce the possibility that one particular day would obscure or overwhelm the data when compositing, a couple of different criteria were developed for tornadoes to be included in the study. If more than one tornado occurred on a given calendar day, the first tornado for the day would always be used. For any of the subsequent tornadoes to be included in the study, they either had to occur within a different synoptic regime (i.e. first tornado was along a warm front, and the second tornado was not associated with a discernable surface boundary), and/or the tornado had to occur 3 hours after the first tornado.

After the final database of significant tornadoes was completed, North American Regional Reanalysis (NARR) data were obtained from the National Climate Data Center's (NCDC) NOAA National Operational Model Archive and Distribution System (NOMADS) website. The NARR dataset is a 32 km 3 hourly regional reanalysis for North America (Mesinger et al. 2005). The three hourly NARR data for the closest time just prior to a particular tornado occurrence was plotted. NARR data was plotted using the General Meteorological Package (GEMPAK; DesJardins 1991).

Using the NARR data, a tornado relative composite grid

---

<sup>1</sup> Corresponding author address: Joshua M. Boustead, 6707 N. 288<sup>th</sup> Street, Valley, NE 68064; email: josh.boustead@noaa.gov

was calculated. This was done by extracting a standard subset of the NARR data. This subset area was centered on the beginning location of the tornado and extended west  $14^\circ$ , east  $7^\circ$ , south  $11^\circ$ , and north  $10^\circ$ . Then the data were averaged by tornado type. Before putting the composited grids into GEMPAK, the data were given the same latitude and longitude, centered on Topeka, KS, for demonstration purposes. The result was a GEMPAK grid where all tornadoes in the study occurred at a latitude and longitude of Topeka, KS. An example of this process is presented in figure 2.

### 3. RESULTS

#### A. Synoptic Overview

The comparison of the 300 hPa analysis is presented in figure 3. The most striking difference is the stronger upper-level jet associated with warm sector significant tornadoes. This may be in response to the propensity of warm sector tornadoes to occur earlier in the spring, but may also signify stronger dynamics are needed for warm sector tornadoes.

There are some noteworthy similarities though. First, the favored location of significant tornadoes is in the left front exit region of the 300 hPa jet. This is a favored area of large-scale ascent associated with the ageostrophic jet circulation. Also of note is that in both synoptic environments, a well defined short-wave trough is upstream of the tornado development, and in both cases the wave is negatively tilted.

Figure 4 is the 500 hPa analysis comparison. Again, the warm sector cases appear to be associated with much stronger wind speeds. In both cases, a thermal trough can be seen, but in the warm sector cases, the thermal trough is displaced upstream of the location of the trough in the height field. This may indicate that many significant tornadoes are associated with a deepening synoptic system. Cold air advection (CAA) is indicated in both frontal and warm sector cases near the location of the significant tornadoes.

The 700 hPa comparison is presented in figure 5. The most noteworthy dissimilarity is the steeper 700 to 500 hPa lapse rates associated with the frontal cases. This may be a product of the later seasonal occurrence of significant tornadoes associated with a discernable surface boundary. Another contributing may be the occurrence of warm air advection (WAA) occurring at 700 hPa in frontal cases, while CAA is taking place in warm sector. There were no situations in the database where warm sector significant tornadoes occurred on days when frontal tornadoes observed. This could indicate a capped warm sector, or if thunderstorms did develop, the ambient shear was not sufficient for significant tornadoes. The wind speed differences at 700 hPa are less than levels above, with wind speeds in both cases at the location of the significant tornadoes between  $10$  and  $20 \text{ m s}^{-1}$ .

A comparison of the 850 hPa composites is presented in figure 6. Tornadoes occur just to the east (southeast) of the low in the frontal (warm sector) cases. In the frontal cases, the tornado typically occurs to the northeast of the warmest 850 hPa temperatures and within the highest dew point maximum. Backed 850 hPa winds of  $10 \text{ m s}^{-1}$  are noted near the location of the tornado. In the warm sector cases, the tornado is occurring on the northwest side of the warmest 850 hPa temperatures and on the western edge of the moisture axis. The 850 hPa winds are slightly veered to west of due south with speeds of  $10$  to  $15 \text{ m s}^{-1}$  noted. In both cases, a dry intrusion at 850 hPa is noted to the southwest of the tornado location, but this is much stronger in the warm sector cases.

The surface analysis comparison is presented in figure 7. Front cases appear to occur to the northeast of the surface low and on the northwest side of the moisture axis with low level flow backed to the southeast. In the warm sector cases the significant tornadoes appear to occur just to the east of the surface low and along the western edge of the moisture axis. Also of note is the sharper temperature gradient along the warm front in the warm sector cases. In contrast, in the front cases, warmer air extends well to the north of the warm front.

#### B. Convective Results

A comparison of 100 hPa mixed layer (ML) convective available potential energy (CAPE) and 0 to 3 km helicity is presented in figure 8. In both cases, around  $150$  to  $175 \text{ m}^{-2} \text{ s}^{-2}$  of helicity are present near the location of the tornado. The most significant difference is the position of the MLCAPE maximum in relation to the tornado occurrence; the frontal cases occur in and just northwest of the maximum, but in the warm sector cases, the tornadoes are occurring on the western edge of the MLCAPE axis.

Results of ML convective inhibition (CIN) are presented in figure 9. As expected, in both cases a relatively low MLCIN of around  $-25 \text{ J kg}^{-1}$  is noted near the location of the tornado. In addition, standard deviation indicates that this value varies in most tornado occurrences by less than  $-25$  to  $-50 \text{ J kg}^{-1}$ , indicating a weakly capped atmosphere with respect to a mixed layer parcel near the location of the tornado.

Point soundings at Topeka, KS of the composite environment support the significant differences on the synoptic scale noted above (Fig. 10). The thermodynamic profile associated with frontal tornadoes is considerably moister throughout the column than the warm sector sounding. There is more instability in frontal cases, due to the steep lapse rates and higher equilibrium level. One of the more striking differences, however, is in the vertical wind profile. In the frontal cases, there is a strongly backed low level wind profile with significant turning noted around 850 hPa. In contrast, in the warm sector cases, there is very little

turning with height, indicating a nearly straight hodograph with much of the shear being in the form of speed shear. Speeds at each level are relatively low with respect to what one may think of for significant tornadoes, but this is likely a result of the composite process.

The 0 to 6 km shear vector was plotted on a surface analysis to analyze the orientation of the vector to possible near-surface forcing mechanisms (Fig 11). Although the data is smoothed due to the composite procedure, a favorable orientation near 45° of the shear vector to what appears to be a dry line is seen in the warm sector cases (Bluestein and Weisman 2000; Dial and Racy 2005), indicating an increased potential to produce discrete supercells. For the frontal cases, the orientation of the composite shear vector to the surface forcing, which in most cases is a boundary in a general west to east orientation (as in the composite surface analysis), is more parallel. This would tend to limit the longevity of the supercells associated with fronts. Indeed, in the database, the average length for a warm sector significant tornado is 24.5 km, while the frontal cases are near 15.9 km.

### C. Statistical Results

Soundings and hodographs were analyzed individually to gather indices which have been shown to be important in the convective environment assessment. Figure 12 gives the thermodynamic comparisons. As indicated in section 3B, the frontal cases are associated with more MLCAPE for most occurrences. More importantly, though, it appears that significant destabilization is occurring on the cool side of the boundary in the frontal cases, allowing for surface-based convection. Both the frontal and warm sector cases have very low MLCIN values, with 75 percent of the cases in both categories having less than  $-20 \text{ j kg}^{-1}$ . Differences are also noted in the level of free convection (LFC) and the lifted condensation level (LCL). The LFC in the warm sector cases show a larger range of values and indicate very few significant tornadoes in the warm sector occur with a LFC less than 1000 m. This is likely due to the lower boundary layer moisture content in the warm sector cases, and this trend continues in the LCL category as well.

Storm relative flow has been shown to be important in storm morphology (Rasmussen and Straka 1998), and the results here agree well with their findings (Fig. 13). In all levels analyzed for the warm sector cases, the 50<sup>th</sup> to 75<sup>th</sup> percentiles of storm relative flow was above  $10 \text{ m s}^{-1}$ . This is likely an indication that significant tornadoes occurring in the warm sector are more likely to happen from classic supercell structures. Storm relative flow supportive of classic supercells was also generally true in the frontal cases, but some indication was also noted in the 0 to 2 km and 4 to 6 km levels that weaker storm relative flow would also favor more of a high precipitation supercell.

Vertical shear, both bulk and cumulative, occurring in either warm sector or frontal cases was sufficient for supercell structures (Weisman and Klemp 1982), although warm sector cases continued to show slightly higher shear values (Fig. 14). More notable findings appear to come from low-level shear. Low-level bulk shear in the 0 to 2 km layer is low for both frontal and warm sector cases when compared to the low-level cumulative shear. For both frontal and warm sector cases, at least  $15 \text{ m s}^{-1}$  of cumulative shear was noted at the 25<sup>th</sup> percentile. This would tend to indicate that a significant amount of speed shear in the lowest 2 km is often occurring during significant tornadoes in both synoptic patterns. Also of interest is the comparison of the 0 to 2 km storm relative helicity (SRH). Larger differences are noted between frontal and warm sector cases than were noted with low-level shear. The mean values of SRH for warm sector (frontal cases) are  $211 (157) \text{ m}^2 \text{ s}^{-2}$ . This is likely in part due to the stronger wind field in the warm sector cases, but also may be an indication of the stronger low-level shear needed to get significant tornadoes in the warm sector without a discernable surface boundary to add horizontal vorticity.

## 4. CONCLUSIONS

Composites of environmental conditions for significant tornadoes occurring with and without discernable surface boundaries were done for eastern Kansas. A database of significant tornadoes was made, and NARR data were obtained for the each tornado occurrence. The composites were completed in a storm relative framework where the NARR data were adjusted so that all initial tornado touchdowns occurred at the same latitude and longitude (Topeka, KS).

Comparisons of significant tornadoes occurring near a discernable surface boundary and without yielded some noteworthy differences and similarities. Warm sector significant tornadoes appear to be associated with a stronger synoptic system, but both frontal and warm sector tornadoes occurred generally in the left front exit region of the upper level jet. Tornadoes with frontal cases generally occurred with WAA at 700 hPa and steeper 700 to 500 hPa lapse rates, while the warm sector cases occurred with 700 hPa CAA and smaller lapse rates. Winds at 850 hPa in frontal cases were strongly backed relative to those in warm sector cases. The tornadoes in the warm sector occurred near the western edge of the 850 hPa moisture axis, while the frontal cases were shown to be well into the deeper moisture. These synoptic findings are summarized in figure 12.

Regarding the convective environment, it appeared the most important items were strong destabilization taking place on the cool side of the boundary in frontal cases, as indicated by the high MLCAPE values on the cool side of the boundary. In addition, both the frontal and warm sector cases indicated little MLCIN. LFC values were higher in the warm sector cases, likely due to the drier environment in which tornadoes in this area occur.

Regarding the kinematic environment, both environments appeared to have sufficient deep layer shear for sustained supercells. Storm relative flow was also favorable for classic supercells, especially in the warm sector cases, but appeared to support both classic and high precipitation supercells in the frontal cases. SRH in the 0 to 2 km layer was stronger in the warm sector, and may be an indication that stronger low-level shear is needed for tornadoes without discernable surface boundaries. Low-level cumulative shear appeared to be important, and values were nearly double that of bulk 0 to 2 km shear. This likely indicates a significant increase in speeds with height is common for significant tornadoes, with much of this shear going to creating streamwise horizontal vorticity.

## References

- Bluestein, H. B. and M. L. Weisman, 2000. The interaction of numerically simulated supercells initialized along lines. *Mon. Wea. Rev.*, **128**, 3128-3149.
- DesJardins, M. L., K. F. Brill, and S. S. Schotz, 1991: GEMPAK5 users guide. NASA Technical Memorandum, 4260 pp. [available from NASA, Code NTT-4, Washington, DC 20546-0001]
- Dial, G. L. and J. P. Racy., 2005. Forecasting short term convective mode and evolution for severe storms initiated along synoptic boundaries. Preprints, *17<sup>th</sup> Conf. on Numerical Weather Prediction*, Washington, DC, Amer. Meteor. Soc.
- Mesinger, F, G. Dimego, E. Kalnay, K. Mitchell, P.C. Shafran, W. Ebisuzaki, D. Jovic, J. Woolen, E. Rodgers, E. H. Berbery, M.B. Ek, Y. Fan, R. Grumbine, W. Higgins, H. Li, Y. Lin, G. Manikin, D. Parrish, and W. Shi., 2005: North American regional reanalysis. *Bull. Amer. Meteor. Soc.*, **87**, 343-360.
- NCDC, 1979-2007: Storm Data. [Available from National Climate Data Center, 151 Patton Ave. Ashville, NC 28801-5001]
- Weisman, M. L. and J. B. Klemp, 1982: The dependence of numerically simulated convective storms on vertical wind shear and buoyancy. *Mon. Wea. Rev.*, **110**, 504-520.

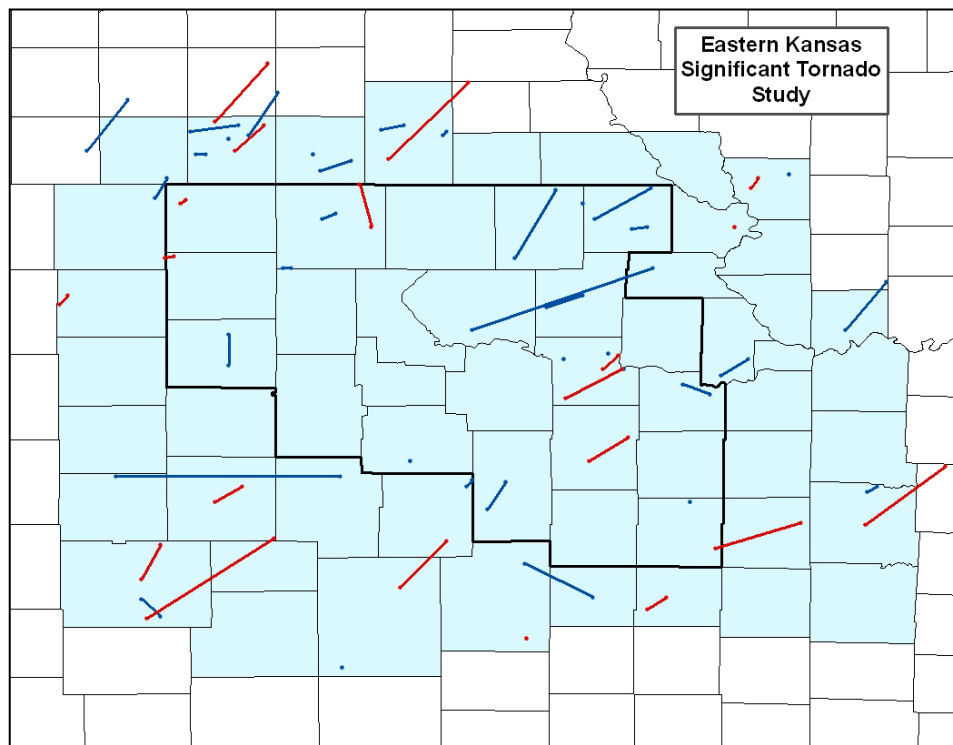


Figure 1. Outline of the study area in light blue. Thick black line outlines the National Weather Service in Topeka, KS warning area responsibility. Tornado tracks are overlaid, warm sector in blue, and frontal in red.

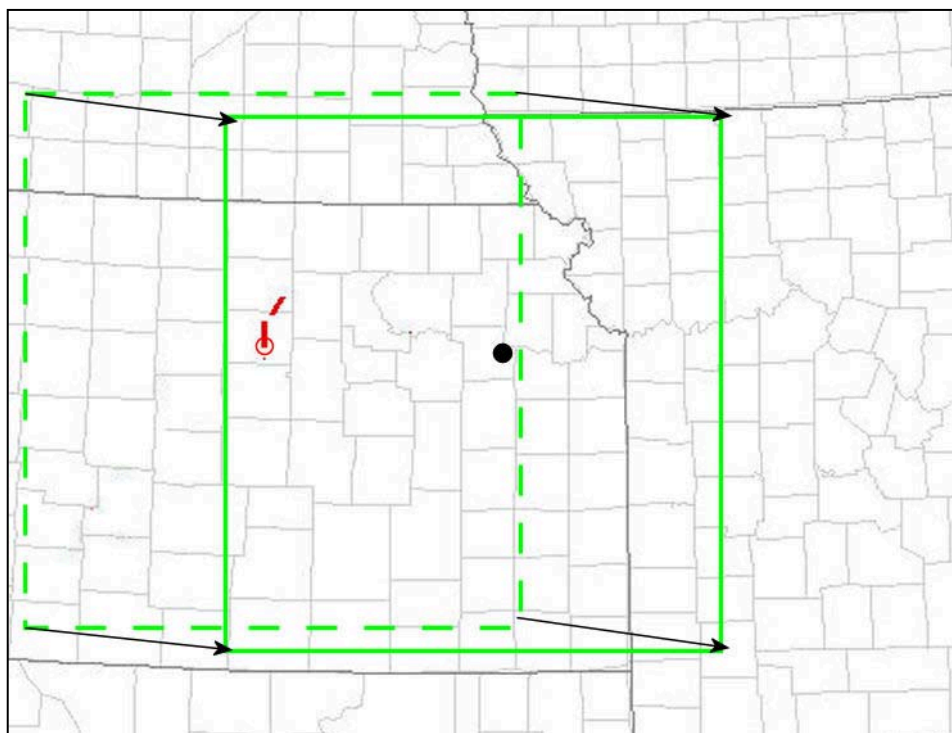


Figure 2. Idealized example of a tornado relative grid. Initial tornado touchdown is used, and a box is drawn around the tornado; that box is then moved such that it is centered over the latitude and longitude of Topeka, KS.

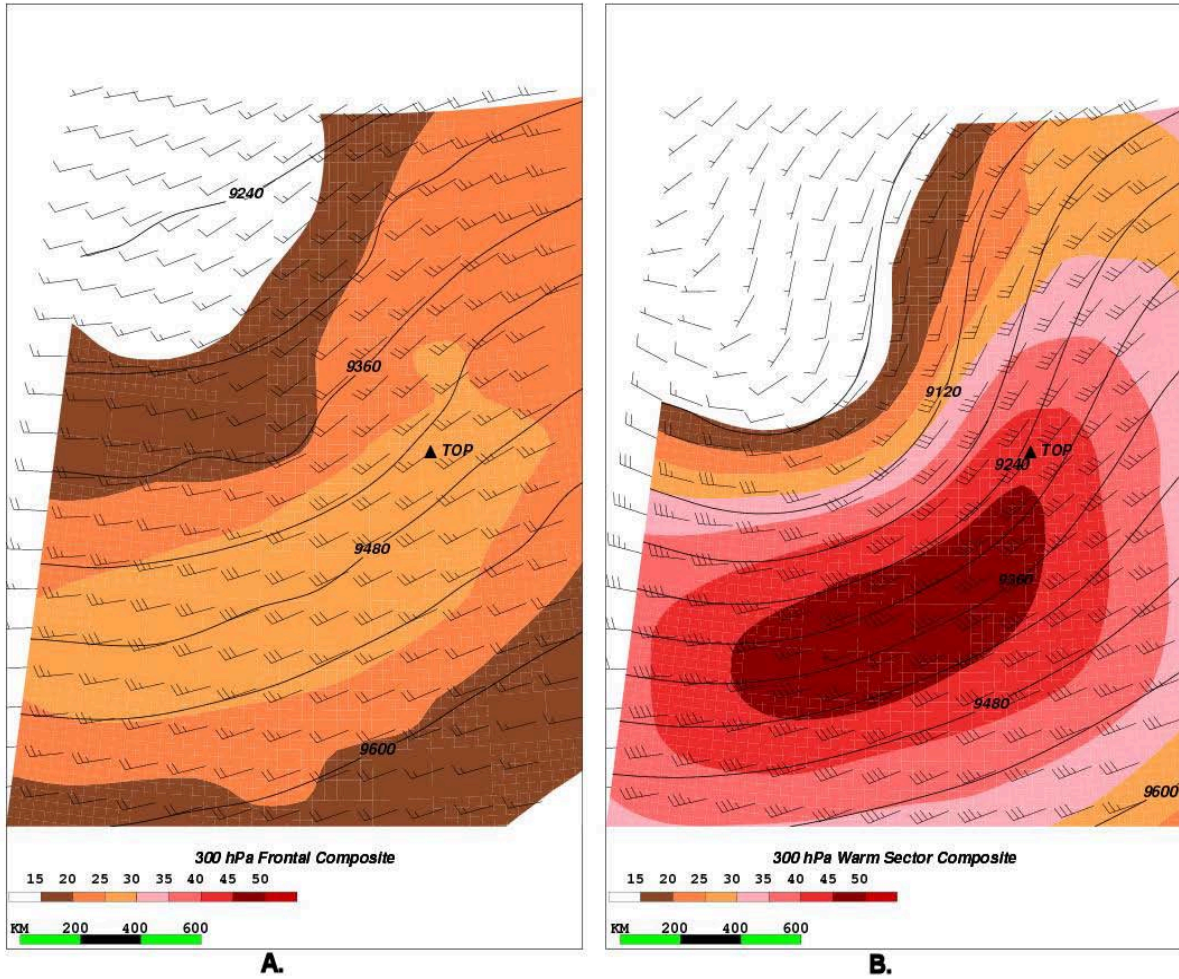


Figure 3. Composite of 300 hPa for front cases (A) and warm sector (B). Thick black contours are heights in meters contoured every 60. Shading is isotachs, and wind barbs are plotted in  $\text{m s}^{-1}$ , half barb  $5 \text{ m s}^{-1}$ , full barb  $10 \text{ m s}^{-1}$ . TOP denotes the tornado observation point in all images.

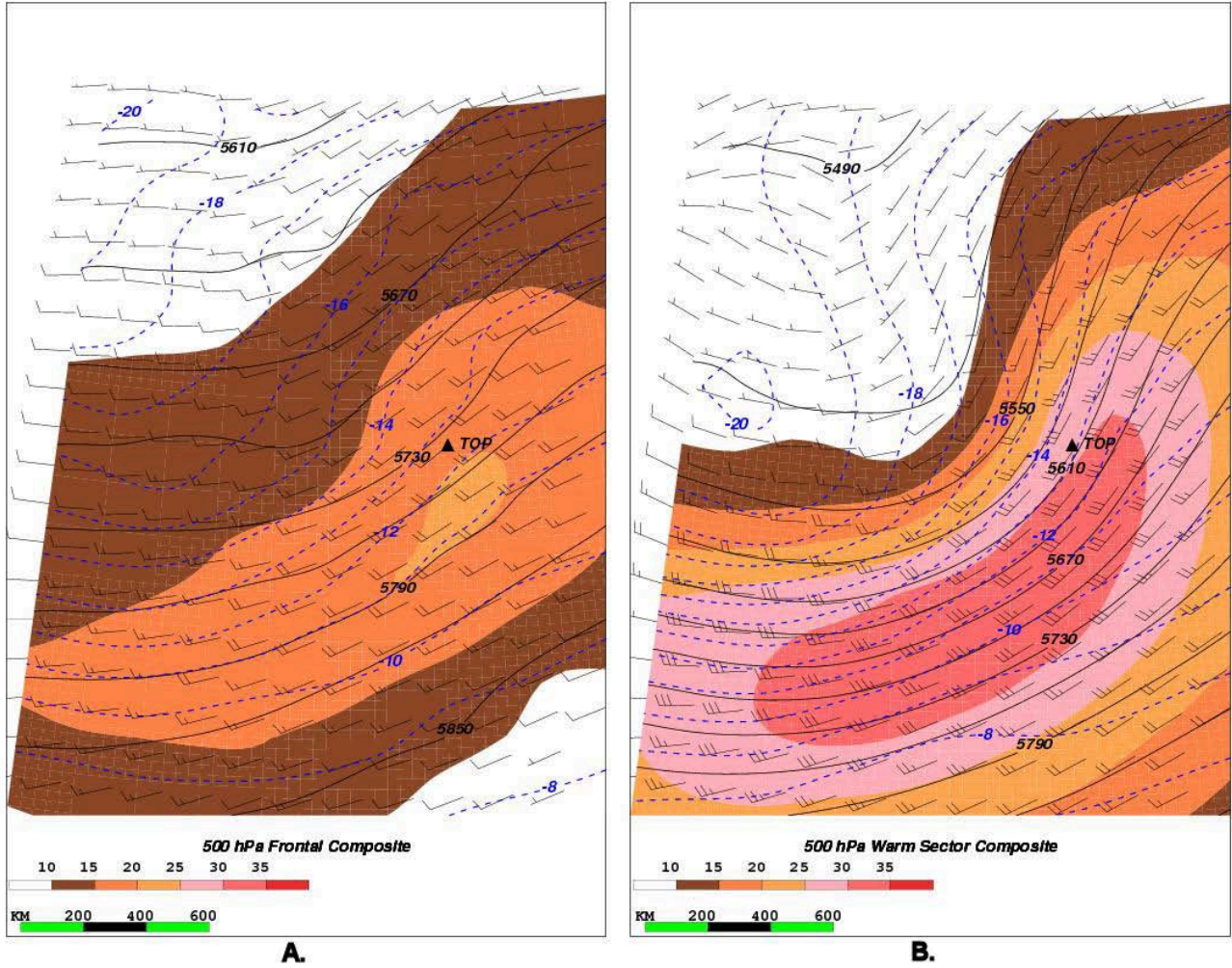


Figure 4. Composite of 500 hPa for front cases (A) and warm sector (B). Thick black contours are heights in meters contoured every 30. Shading is isotachs, and wind barbs are plotted in  $\text{m s}^{-1}$ , half barb  $5 \text{ m s}^{-1}$ , full barb  $10 \text{ m s}^{-1}$ . Dashed blue lines are temperature contoured  $1 \text{ }^\circ\text{C}$ . TOP denotes the tornado observation point.

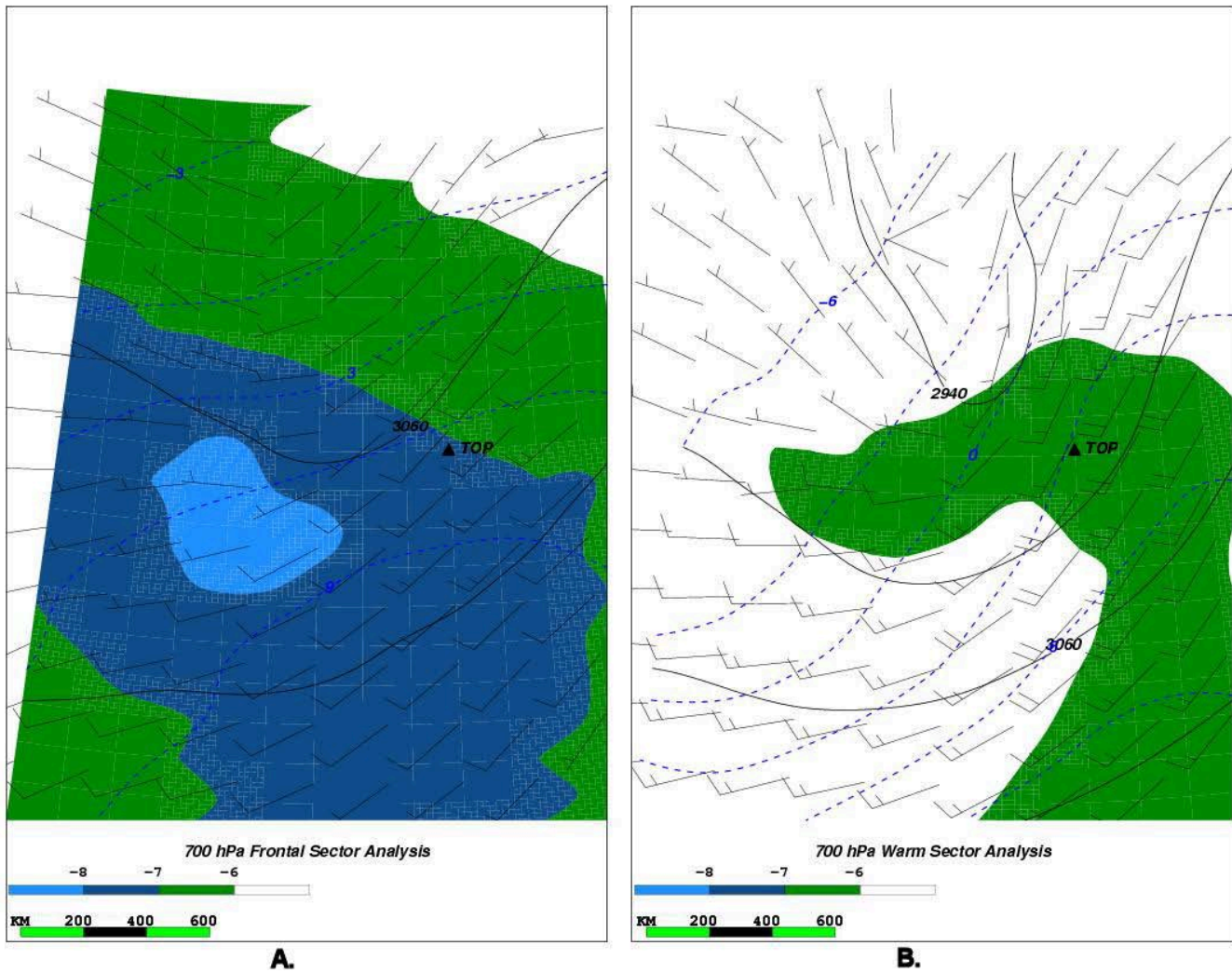
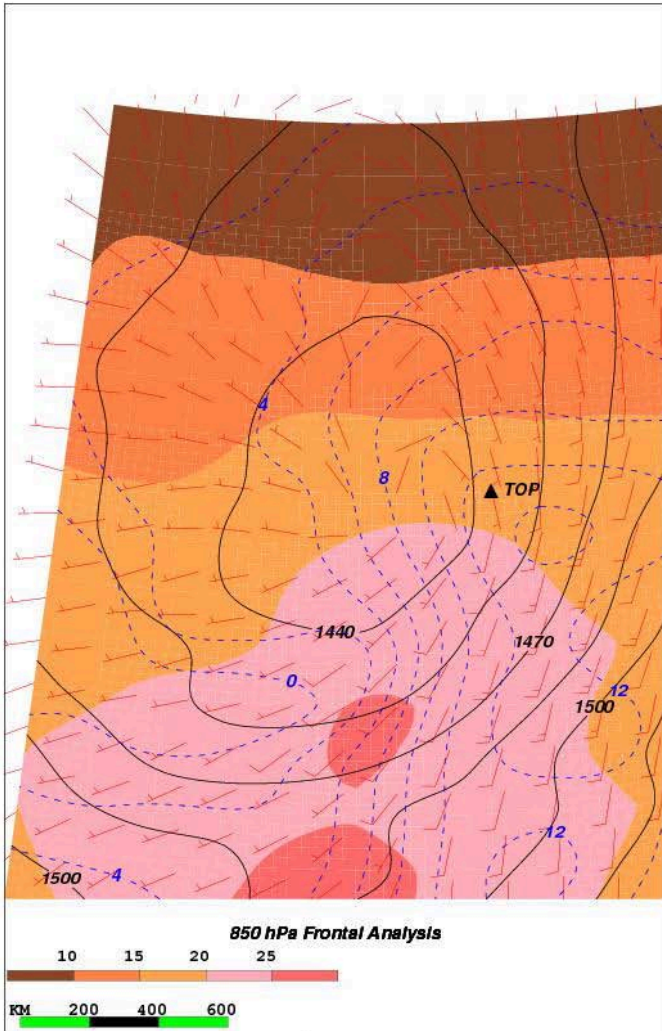
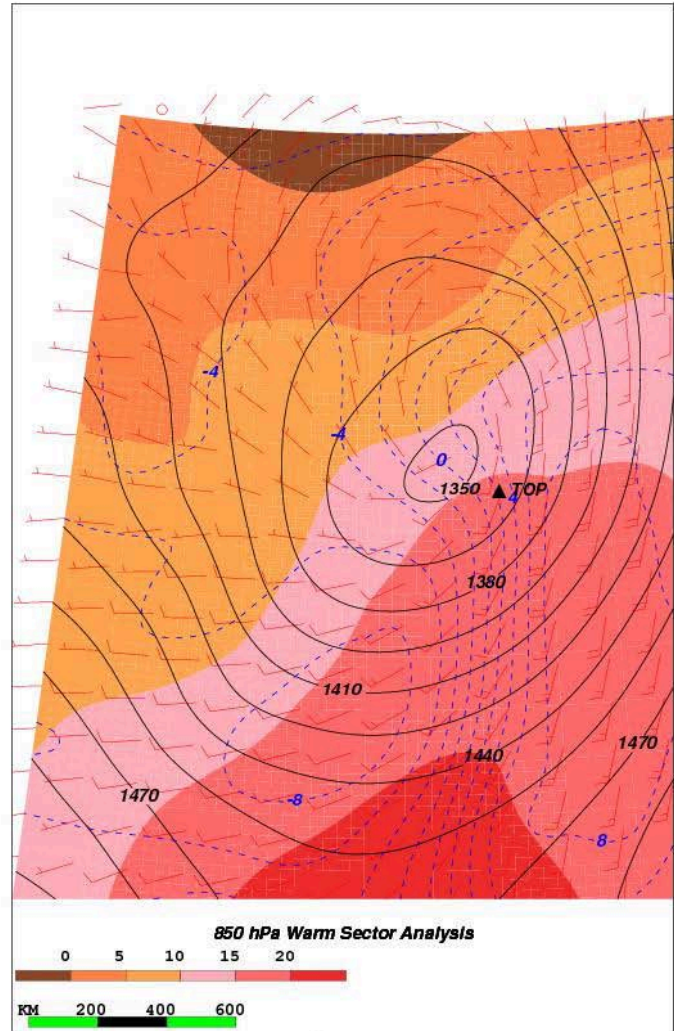


Figure 5. Composite of 700 hPa for front cases (A) and warm sector (B). Thick black contours are heights in meters contoured every 30. Shading is 700 to 500 hPa lapse rates, and wind barbs are plotted in  $\text{m s}^{-1}$ , half barb  $5 \text{ m s}^{-1}$ , full barb  $10 \text{ m s}^{-1}$ . Dashed blue lines are temperature contoured  $3^\circ\text{C}$ . TOP denotes the tornado observation point.



**A.**



**B.**

Figure 6. Composite of 850 hPa for front cases (A) and warm sector (B). Thick black contours are heights in meters contoured every 30. Shading is temperature 5 °C. Wind barbs are plotted in  $m s^{-1}$ , half barb 5  $m s^{-1}$ , full barb 10  $m s^{-1}$ . Dashed blue lines are dew point contoured 2 °C. TOP denotes the tornado observation point.

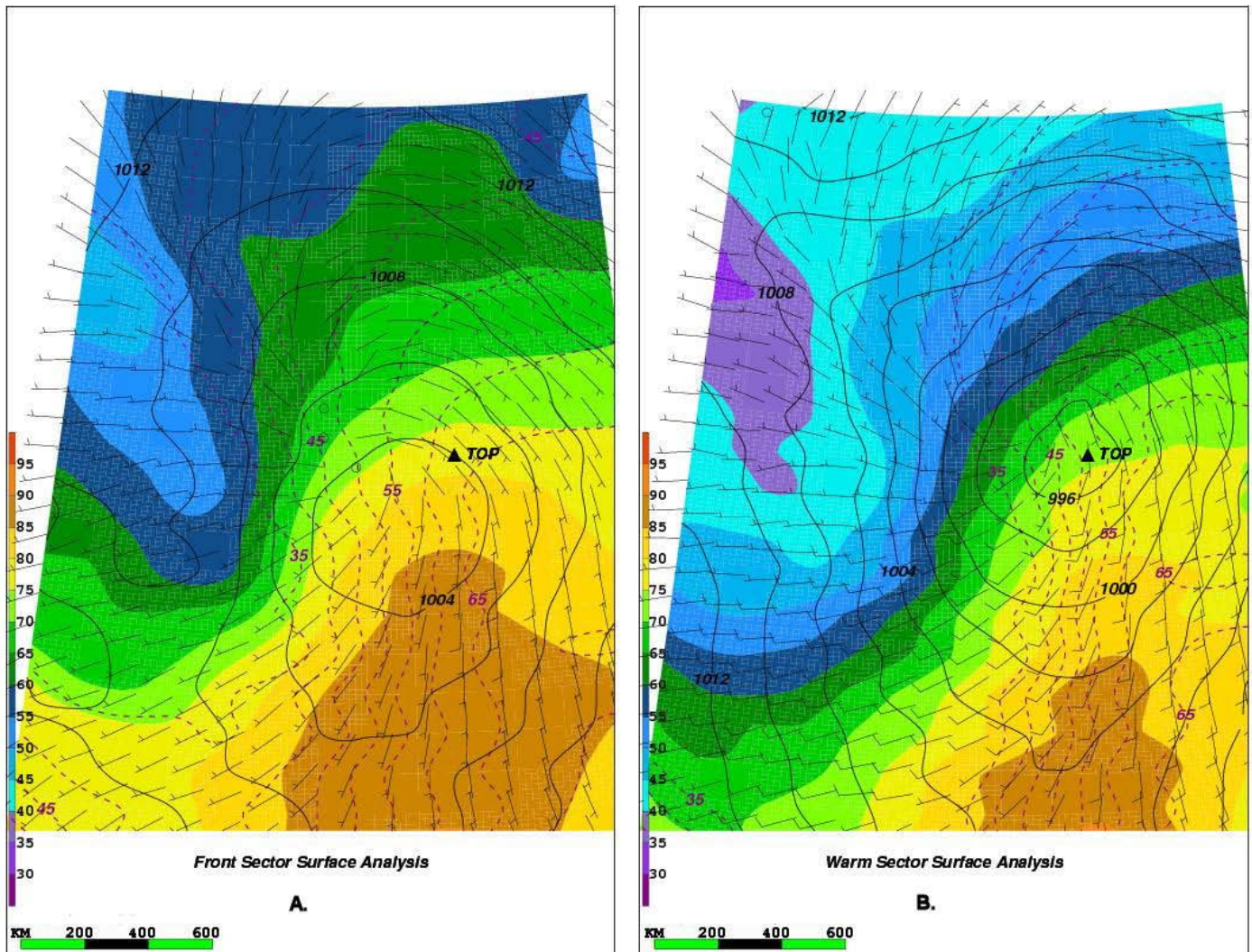


Figure 7. Surface composite for front cases (A) and warm sector (B). Thick black contours are mean see level pressure contoured every 2 hPa. Shading is temperature 5 °C. Wind bars are plotted in  $\text{m s}^{-1}$ , half barb  $5 \text{ m s}^{-1}$ , full barb  $10 \text{ m s}^{-1}$ . Dashed blue lines are dew point contoured 5 °C. TOP denotes the tornado observation point.

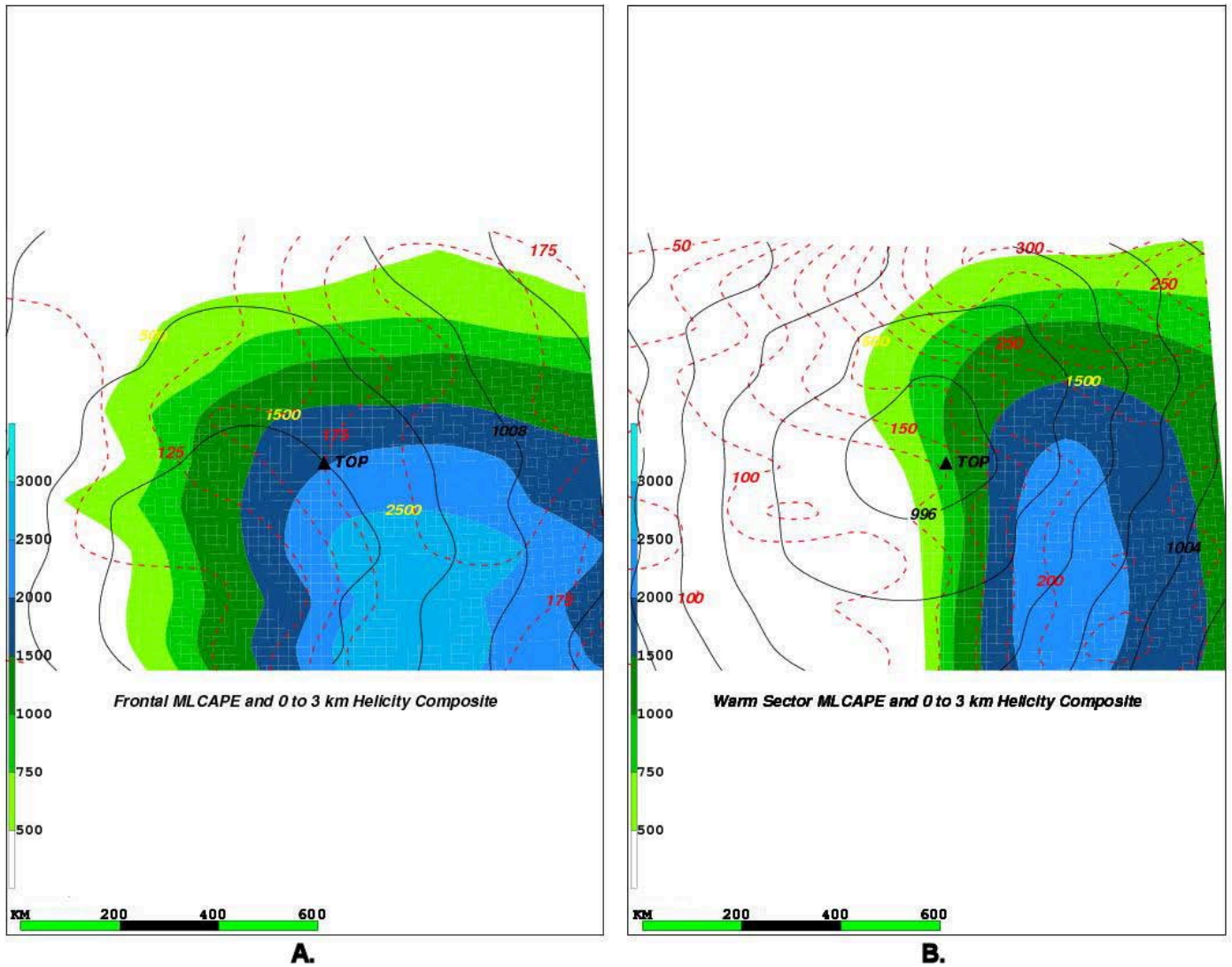


Figure 8. Composite of MLCAPE and 0 to 3 km helicity for front cases (A) and warm sector (B). Thick black contours are mean sea level pressure contoured every 2 hPa. Shading is temperature MLCAPE  $250 \text{ j kg}^{-1}$ . Wind barbs are plotted in  $\text{m s}^{-1}$ , half barb  $5 \text{ m s}^{-1}$ , full barb  $10 \text{ m s}^{-1}$ . Dashed blue lines are helicity contoured  $25 \text{ m}^2 \text{ s}^{-2}$ . TOP denotes the tornado observation point.

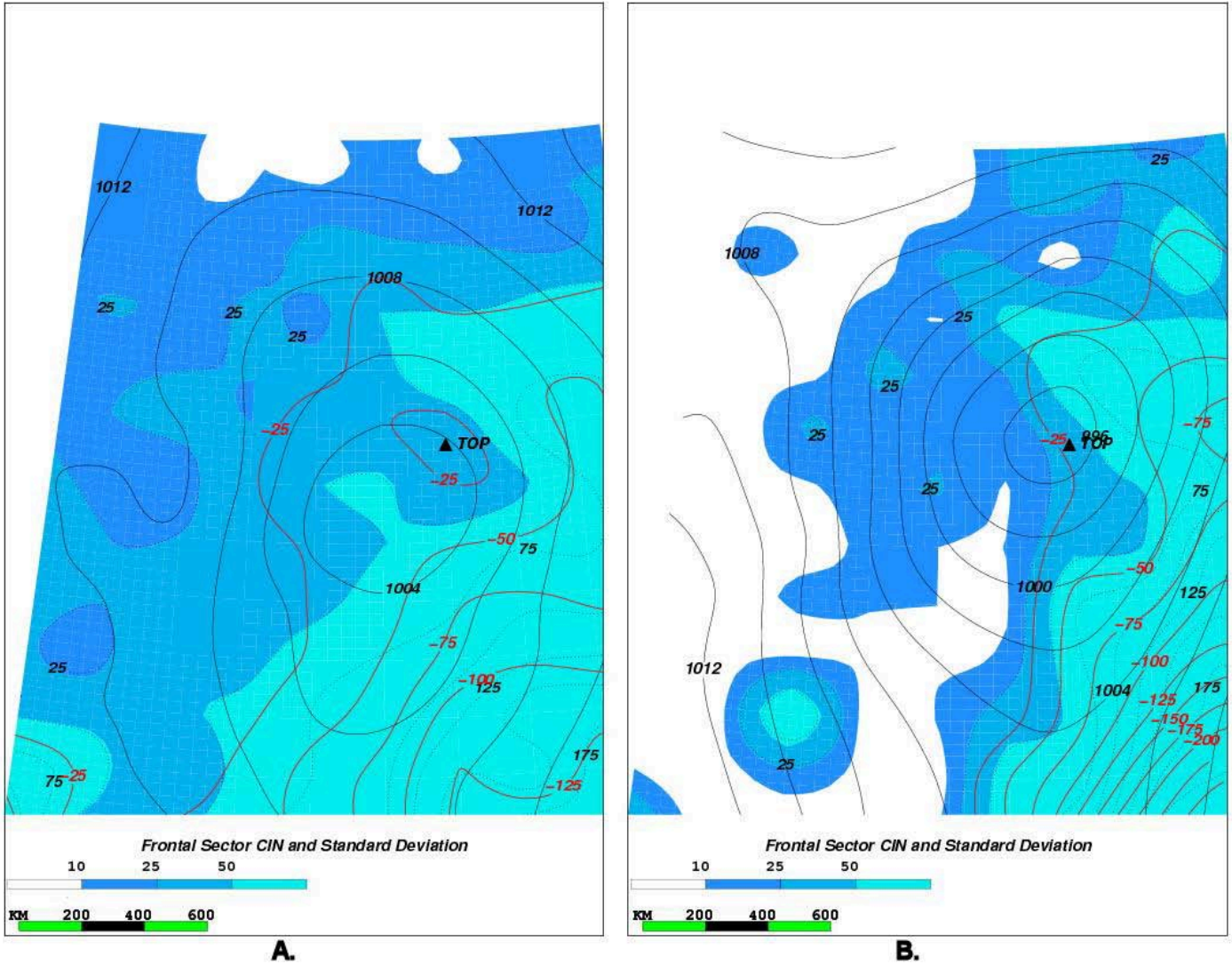


Figure 9. Composite of MLCIN and standard deviation for front cases (A) and warm sector (B). Thick black contours are mean sea level pressure contoured every 2 hPa. Shading is MLCIN standard deviation every  $25 \text{ J kg}^{-1}$ . Dashed lines are MLCIN contoured every  $25 \text{ J kg}^{-1}$ . Wind barbs are plotted in  $\text{m s}^{-1}$ , half barb  $5 \text{ m s}^{-1}$ , full barb  $10 \text{ m s}^{-1}$ . TOP denotes the tornado observation point.

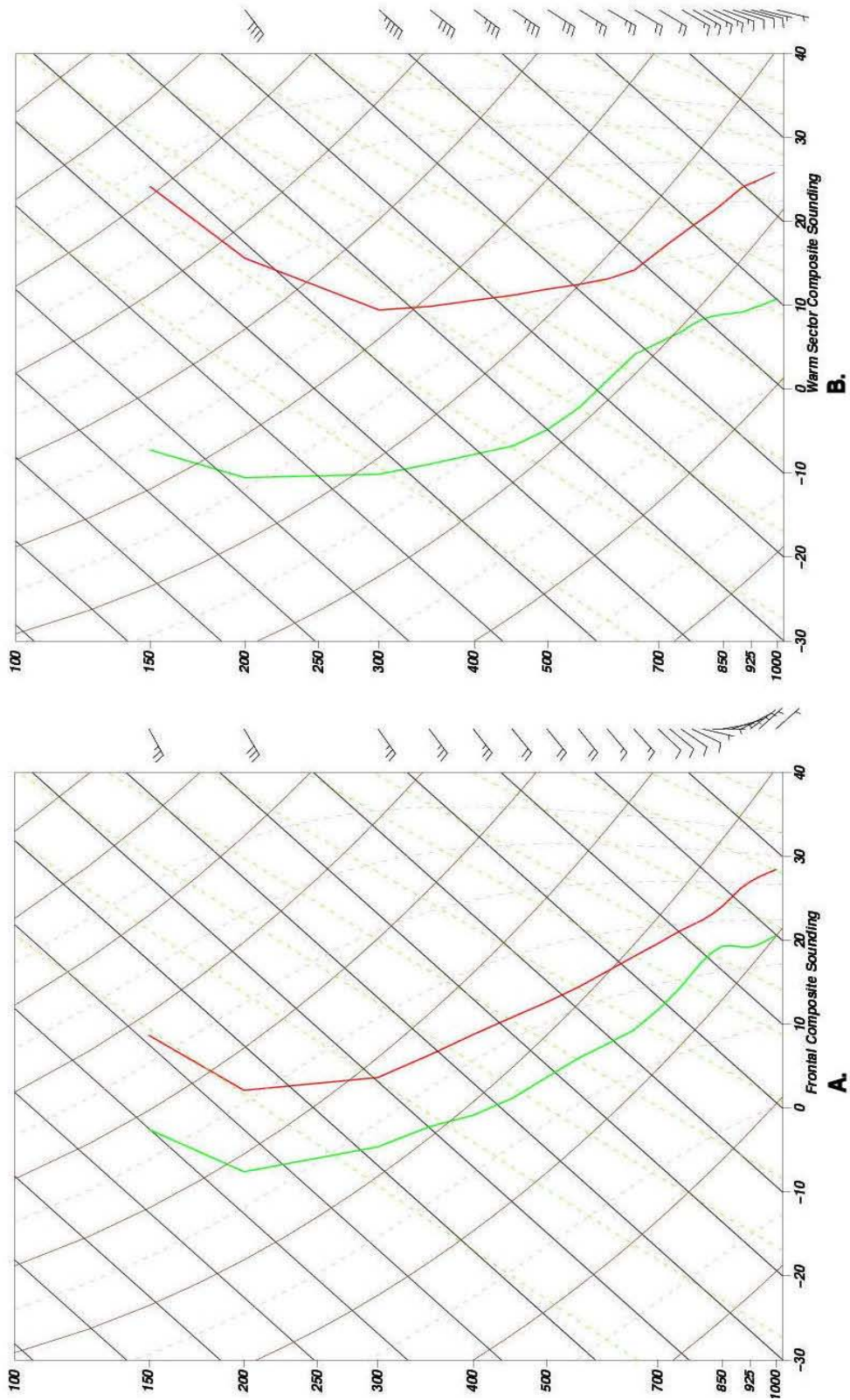


Figure 10. Composite soundings from front cases (A) and warm sector (B). Temperature is in red, and dew point is in green. Wind barbs are plotted in  $\text{m s}^{-1}$ , half barb  $5 \text{ m s}^{-1}$ , full barb  $10 \text{ m s}^{-1}$ .

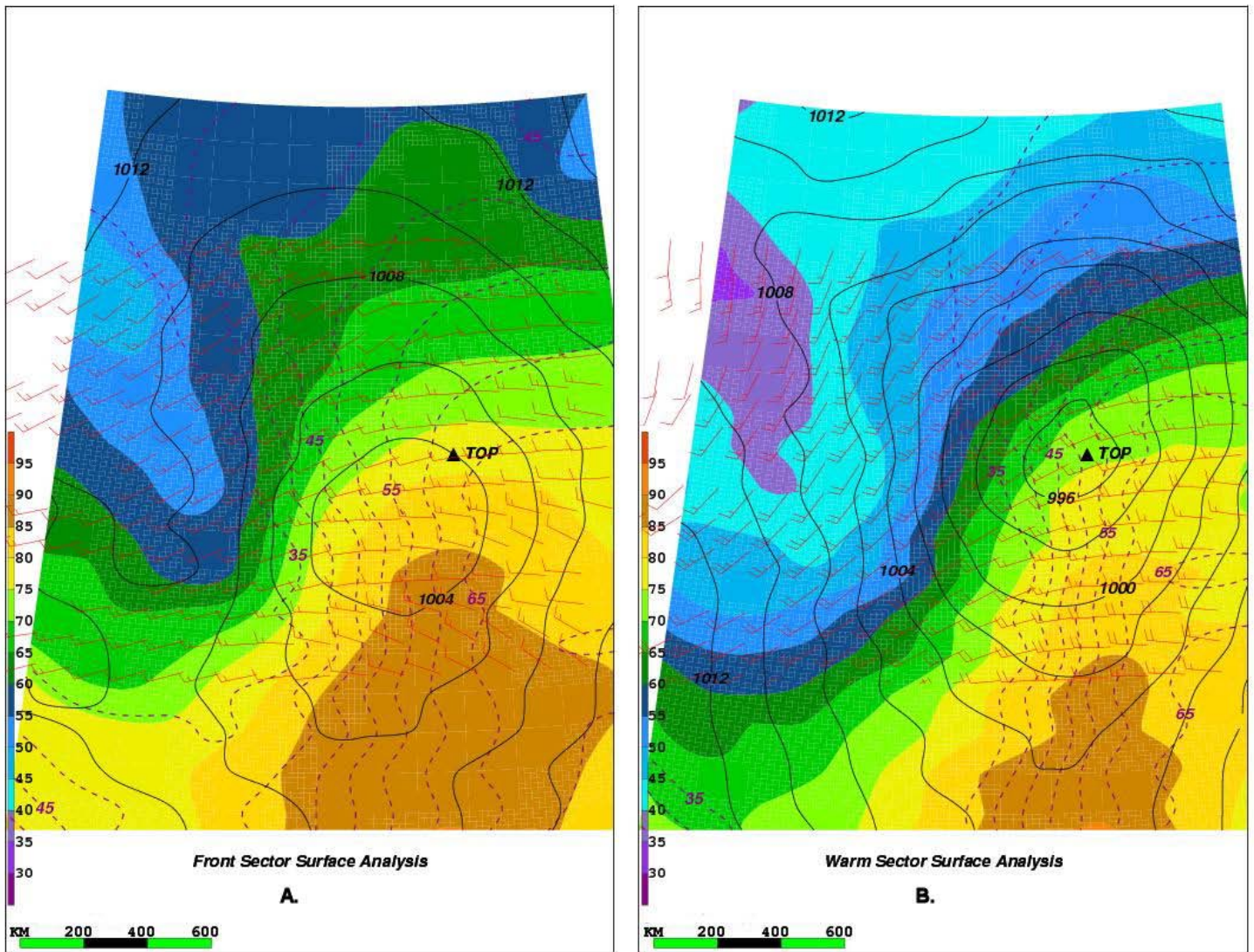


Figure 11. Surface composite for front cases (A) and warm sector (B) with 1 km to 6 km bulk shear vector. Thick black contours are mean sea level pressure contoured every 2 hPa. Shading is temperature 5 °C. Bulk shear vectors from 1 km to 6 km are plotted in m s<sup>-1</sup>, half barb 5 m s<sup>-1</sup>, full barb 10 m s<sup>-1</sup>. Dashed blue lines are dew point contoured 5 °C. TOP denotes the tornado observation point.

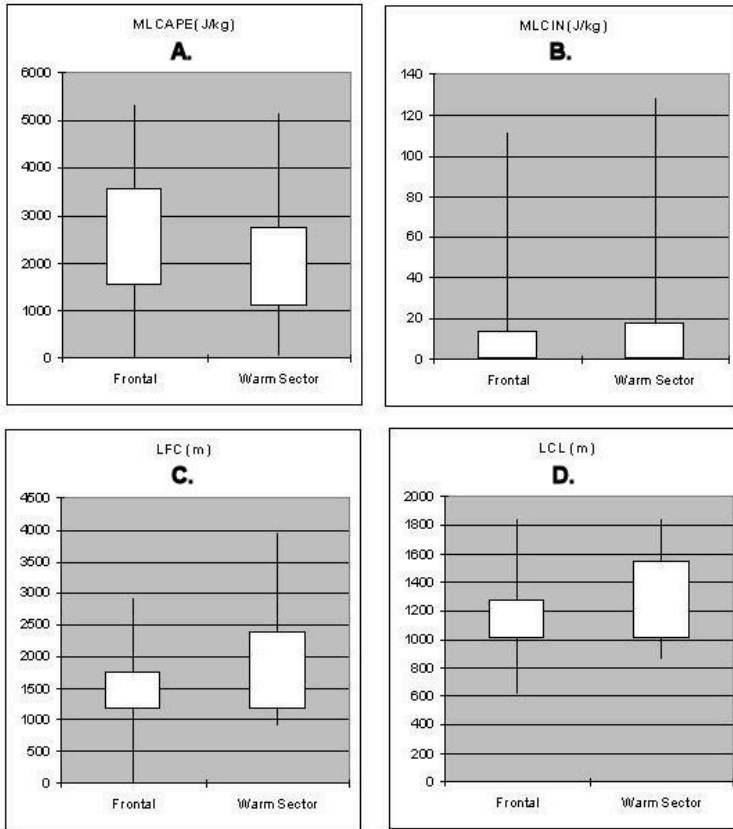


Figure 12. Distribution of MLCAPE in  $\text{J kg}^{-1}$  (A), MLCIN in  $\text{J kg}^{-1}$  (B), LFC in meters (C), and LCL in meters (D). Range of values is represented by solid line, and the 25<sup>th</sup> to 75<sup>th</sup> percentile values are depicted by the shaded box.

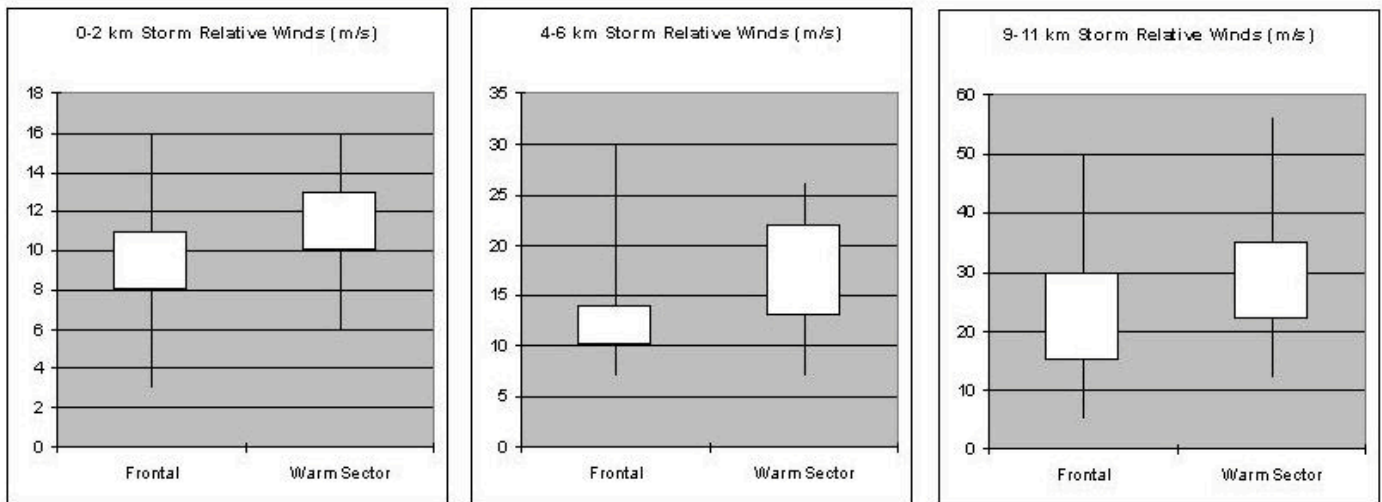


Figure 13. Distribution of storm relative winds in the 0 to 2 km layer (A), 4 to 6 km layer (B), and 9 to 11 km layer (C). Range of values is represented by solid line, and the 25<sup>th</sup> to 75<sup>th</sup> percentile values are depicted by the shaded box.

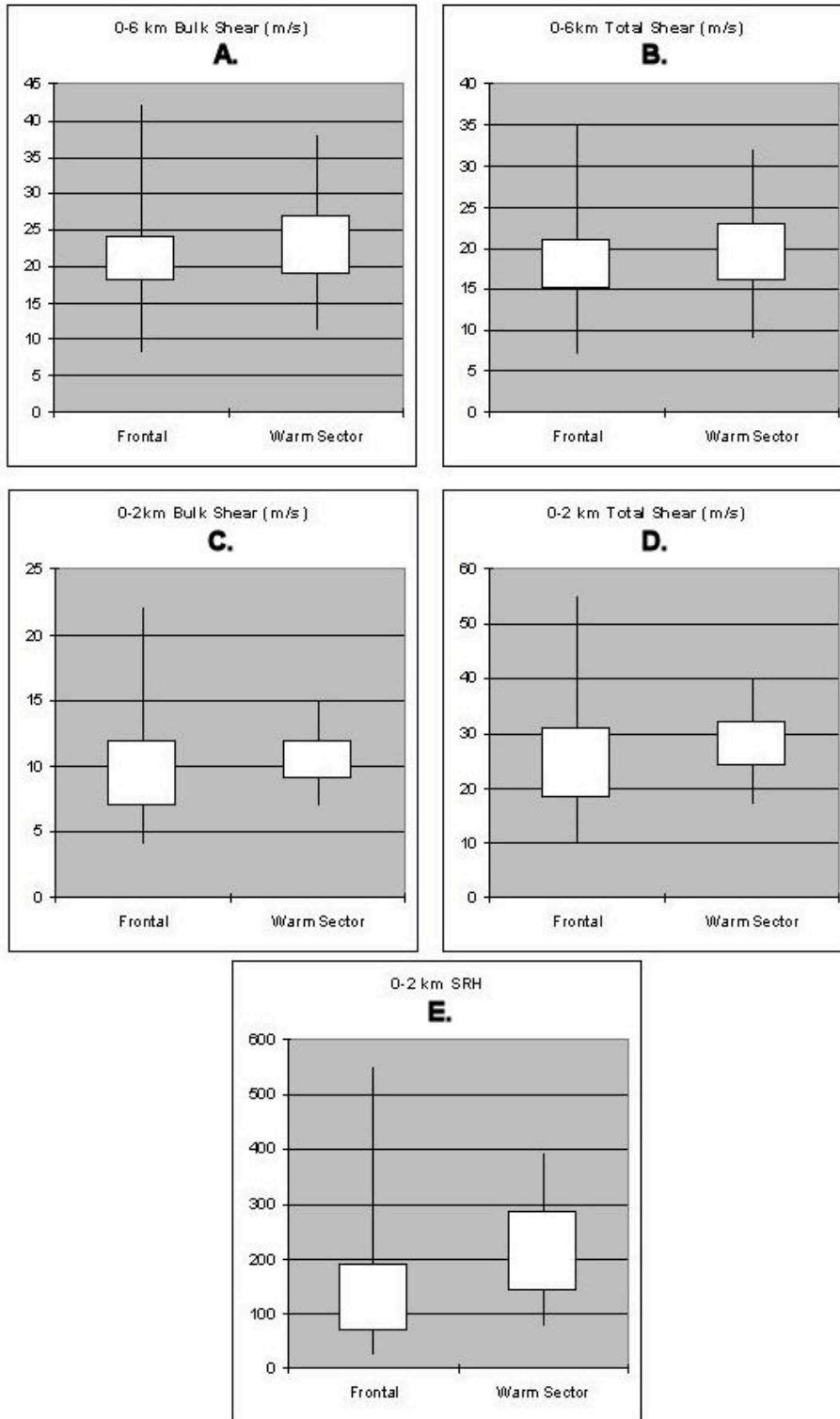


Figure 14. Distribution of 0 to 6 km bulk shear (A), 0 to 6 km cumulative shear (B), 0 to 2 km bulk shear (C), 0 to 2 km cumulative shear (D) all in  $m s^{-1}$ , and 0 to 2 km SRH (E) in  $m^2 s^{-2}$ . Range of values is represented by solid line, and the 25<sup>th</sup> to 75<sup>th</sup> percentile values are depicted by the shaded box.

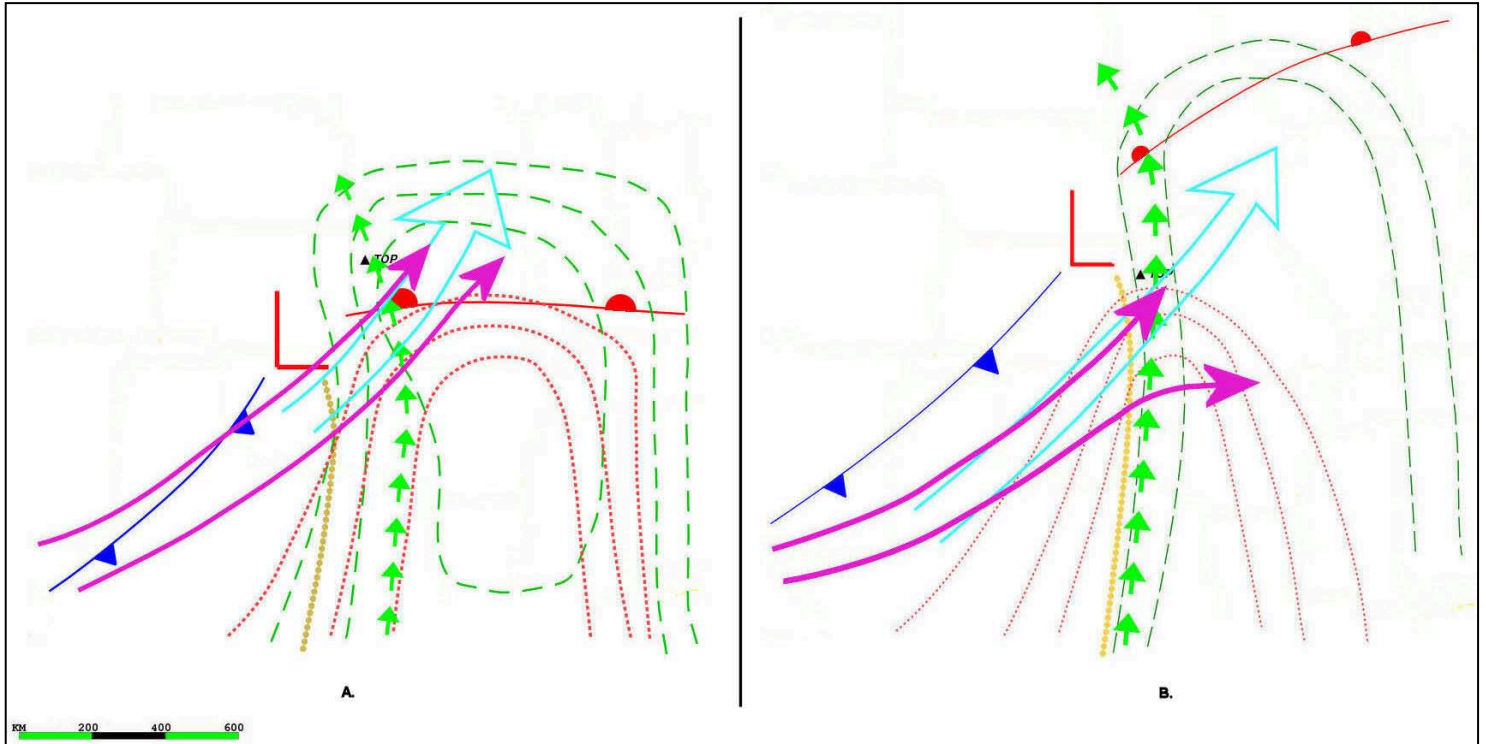


Figure 15. Idealized synoptic pattern associated with significant tornadoes associated with a front (A) and in the warm sector (B). Surface pattern is plotted with conventional fronts. Surface dew points are plotted in dashed lines, and temperature is plotted in dotted lines. The 850 hPa jet is plotted with large green arrows. The 700 and 500 hpa jet is plotted in the light blue arrow, and the 300 hPa jet is plotted in the thick purple arrows.